GRC Transactions, Vol. 42, 2018

Addressing Clogging Risks When Injecting Geothermal Water in Sandstone Aquifers: Lessons Learnt in Australia

Martin Pujol[1], Miranda Taylor[1], Steve Bolton[1], Grant Bolton[1], Ian Brandes de Roos[1] and Jeff Dusting[2]

Rockwater[1], Norman Disney and Young[2]

Keywords

Geothermal, sandstone, injection, clogging, direct-use, filtering, completion

ABSTRACT

Injection of geothermal water into aquifers composed of interbedded sandstone, siltstone and shale can be challenging. In particular, clogging issues have impeded the development of many clastic geothermal resources globally. The following have been cited as causes of clogging: suspended solids and/or gas bubbles in the water, proliferation of bacteria, chemical precipitation in the water and/or in the aquifer, swelling and dispersion of clays and fine sediment migration and plugging of the aquifer.

While the main causes of clogging have been studied by researchers and been the subject of a number of successful pilot-scale studies for decades, scarce published information exists regarding the key technical solutions and procedures that have guaranteed the success of injection into sandstone aquifers in modern industrial applications.

Geothermal electricity production in Australia is still in its infancy; however direct-use applications, mainly for municipal pool heating have had an exponential growth over the last 20 years in Western Australia (WA) with 14 projects in operation (i.e. a total of 28 bores). The economics of these direct-use projects are sensitive to parasitic energy losses associated with injection of heat-depleted water. This has resulted in significant research effort to address clogging mechanisms. The success of projects in WA has inspired projects in other states of Australia particularly in Victoria.

This paper focuses on seven selected Australian projects involving injection into sandstone aquifers where the authors have had firsthand involvement. Issues discussed will include clogging associated with suspended solids and chemical precipitation. Additionally, the key design criteria that have permitted successful economic injection of heat-depleted groundwater into sandstone aquifers are discussed.

1. Introduction

Perth is the capital and largest city of the Australian state of Western Australia (WA) with an estimated population of about 2.1 million in the greater Perth area. Perth is also one of the highest water using cities in Australia: the average person using about 130×10^{3} L $year^{-1}$ of scheme water at home.

Groundwater provides almost half of the city's metropolitan water supply, with about a third of this is sourced from the Yarragadee aquifer – an extensive, confined aquifer that extends across most of the Perth Basin from about 400-600 m depth underneath Perth (Davidson and Yu, 2008).

Geothermal direct-use heating has developed in the Perth Basin since the early 20^{th} century, coinciding with the exploitation of the Yarragadee aquifer for water supply. The first (now obsolete) direct-use applications included heating of the reptile enclosure at the Perth Zoological Gardens (circa 1898), water heating at the Claremont laundry (circa 1940's), wool scouring in Jandakot and opportunistic bathing applications (for example the popular Tawarri warm baths) (Pujol et al., 2015). All of these applications relied on a single geothermal bore with surface discharge and reuse of the heat-depleted water.

The first bore targeting the Yarragadee aquifer solely for geothermal heat production was drilled in 1998 in Bicton. There are now thirteen other direct-use geothermal projects which have targeted the Yarragadee aquifer operating in the Greater Perth area. These projects are primarily for heating of pools and space in large leisure centres.

As the aquifer is also exploited for water supply and has experiencing significant pressure decline, it has become a regulatory requirement over the last 15-20 years to inject all heat-depleted groundwater back into the source aquifer after it passes through a heat-exchanger. The water is returned via injection bores targeting the upper part of the aquifer.

Overall, severe clogging issues that have impeded the development of many clastic geothermal resources globally have been largely avoided. However, some projects have required regular injection bore cleaning workovers to maintain good injectivity values and thus, lower operating costs. Until now, there haven't been any guidelines published to quantitatively assess clogging risks and subsequently enable a proponent to determine the likely frequencies of workovers. This directly impacts the operating costs of a project

There is little published information regarding the key technical parameters and solutions that have guaranteed successful injection into the Yarragadee sandstone aquifer in Perth. This paper assesses, correlations between bore design parameters, surface filtering design parameters, aquifer parameters and clogging rates, using data from seven of Perth's previously unpublished operating geothermal projects (i.e. a total of 14 bores). The reader may refer to Appendix I for key bore and aquifer data. Bores 1 to 7 are injection bores while Bores 8 to 14 are production bores.

2. Hydrogeology of the Yarragadee aquifer

Amongst the uppermost stratigraphic units exhibiting aquifer properties beneath Perth, only the mid-Jurassic (Bathonian) clastic sedimentary rocks of the Yarragadee Formation contain sufficiently warm groundwater (i.e. at a temperature of 40°C or more) for geothermal direct-use projects (Pujol et al., 2015). Deeper geothermal targets exists but have not been explored for geothermal applications.

In the Perth area, the Yarragadee aquifer occurs from about 400 to 600 m depth and probably extends to 1800-2000 m depth (Davidson and Yu, 2008). A detailed description of the Yarragadee aquifer is presented in Davidson (1995), Davidson and Yu (2008), Timms et al. (2012) and Delle Piane et al. (2013). Further unpublished data are provided in this paper based on data from the projects described.

2.1 Lithological description and depositional environment

Yarragadee sediments were probably laid down in a fluvial environment (Davidson and Yu, 2008) in the form of a vegetated floodplain traversed by meandering rivers (Tait, 2008).

Timms et al. (2012) used sedimentary logging on cores from Cockburn-1 (the only onshore oil exploration well drilled near Perth) to develop a lithofacies scheme for the Yarragadee Formation. They found that the Yarragadee sediments could be grouped in three main facies: (1) a fining-up sequence of coarse- and medium-grained sandstones of high to moderate energy; (2) fine-grained sandstones and floodplain paleosols; and (3) carbonaceous swampy deposits.

For the purpose of this paper it is considered that the only sediments conducive to geothermal fluid production and injection are the bottom 70-80% of the fining-up sandstone beds. For the purpose of this paper, the net aquifer thicknesses of sandstone beds (h) were estimated from wireline Gamma Ray (GR) for the selected 14 bores. All GR logs were re-scaled so that clean sands had a reading of 30 API and pure shales had a reading of 150 API. An empirical GR cutoff of 60 API was used to estimate the net aquifer thickness for each bore. The net aquifer thicknesses range from 33 to 144 m for the selected bores.

2.2 Aquifer geometry

The formation is very sandy in some of the studied bores (up to 70% of the gross thickness) and considerably less in others (down to 35%). Davidson and Yu (2008) estimate that on average the Yarragadee Formation is made up of approximately 50% sandstone. The average net aquifer thickness estimated for the 14 studied bores is similar (52%).

(a) 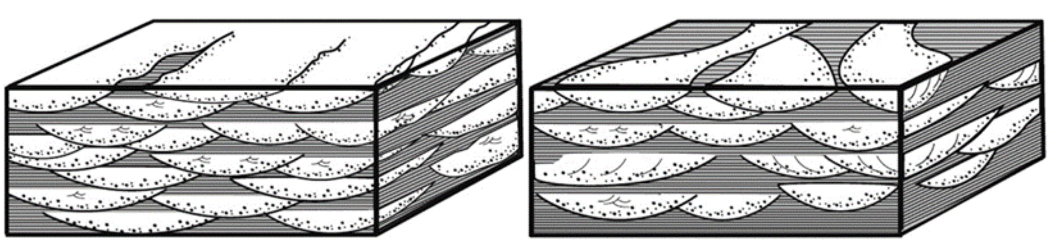 (b)

Figure 1: Higher (a) and Lower (b) net aquifer thickness in a fluvial environment of deposition (modified from Corbett et al, 2012)

In the sandier areas (see Figure 1a), the aquifer is a complex of vertically and laterally stacked and apparently interconnected sandstone beds with discontinuous eroded remnants of the originally extensive floodplain deposits. In the less sandy areas, many of the sandstone beds may be isolated by floodplain sediments (see Figure 1b). The seal quality of the floodplain sediments is variable from "poor" to "good" (Tait, 2008). Locally the floodplain sediments may form aquitard layers and can retard vertical groundwater flow between sandstone beds resulting in vertical potentiometric head and salinity gradients within the aquifer. Most geothermal projects make use of this; by setting the injection bore screens in prospective sandstone beds above a significant shale interval while production screens are set in another sandstone bed below the shale (see Section 3). The low vertical permeability of the interbedded fine-grained clastics minimize the potential for thermal breakthrough between the production and injection bores.

In the sandier bores the fining-up sandstone beds are up to 30 m thick while they are 10 m thick in less sandy bores. Tait (2008) analysed GR profiles of oil exploration wells drilled through the Yarragadee aquifer and found that the sandstone beds can reach up to 45 m thickness in the sandier areas consistent with river channels up to 2 km wide which would have produced meander belts 1.5-20 km wide.

2.3 Mineralogy

Yarragadee Formation mineralogy is primarily controlled by lithological changes with depth (ie. interbedded sandstone, siltstone and shale).

The sandstones have a framework of quartz (approx. 80%) and feldspar (approx. 15%) as demonstrated by Timms et al. (2012) consistent with unpublished analyses on drill cuttings collected during the drilling of selected geothermal bores. Traces minerals (less than 1%) commonly identified by X-ray diffractions techniques include pyrite, mica and siderite. Up to 5% garnet is also reported locally throughout the aquifer (Tait, 2008) but overall concentrations are low. There is a general aluminosilicate enrichment and quartz is less common in finer-grained sediments, with swamp deposits dominated by kaolinite (approx. 55%).

Below 1000 to 1500 m depth, the sediment maximum porosity packing limit of about 30% is attained and thereafter porosity diminishes as a result of quartz cementation (Tait, 2008). The injection bores in this study are all sited shallower than 1000 m depth and are therefore not likely to be affected by porosity loss. In the selected production bores (up to 1150 m depth), a decrease of porosity with depth is not apparent.

2.3 Particle Size Distribution

Yarragadee Formation core's Particle Size Distribution (PSD) data (unpublished) suggest a median particle size (D_{50}) of the sandstone beds (including finer-grained sandstone at the top of the fining up sandstone beds) of about 300-350 microns while the D_{50} of the net aquifer (bottom 70-80% of the sandstone beds) is greater, probably about 400-500 microns.

No core was acquired when drilling the selected 14 geothermal bores. However, PSD analyses were undertaken on the drill cuttings to enable the selection of the wire-wound screen (completion) aperture sizes. Most projects have used dry sieve analyses methods.

Limitations of the method include: (1) dry sieves cannot assess particles finer than 64 microns; (2) the method may underestimate fines' concentrations due to electrostatic adherence with larger grains and losses within the edges of the sieves; and (3) the method may overestimate coarse-grains' concentrations due to the prevalence of residual dried drilling mud to form agglomerating particles.

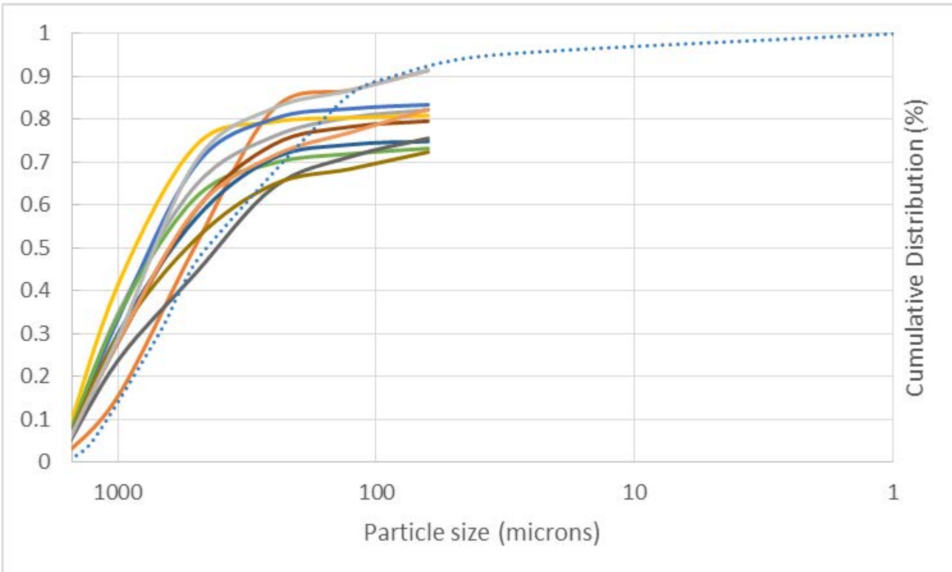

Figure 2: Comparison of field dry sieve analyses (solid) with laser diffraction average analyses (round dot)

To assess the accuracy of the dry sieving analyses method, the dry sieve PSD data from a selected bore (Bore 13, drilled in 2017) are compared with average laser diffraction PSD data for the same interval.

This comparison suggests a general agreement with larger grain sizes; a slight over-estimation of the D_{50} when calculated with the dry sieving method (ie 642 microns and 454 microns respectively); and an unreliable D_{90} when calculated with the dry sieving methods. The implication on the sand control design and clogging is discussed further in Section 3.

However, the accuracy of both the laser diffraction and dry sieving methods are governed by the quality of drill cuttings. Ideally, and where possible, core samples should be used for PSD and dry sieving analyses.

2.4 Hydraulic properties

In order to maintain independence of fluid properties, intrinsic permeability (k) is used in this paper with units of milliDarcy (mD). The hydraulic conductivity conversion is shown in Equation (1).

$$k = \frac{K}{3600 \times 24} \frac{\mu}{\rho g} \frac{1000}{9.869233 \times 10^{-10}} \quad (1)$$

where k, K, μ, ρ and g are absolute permeability (mD), hydraulic conductivity (m/d), fluid viscosity (cP), fluid density (kg/m^3) and acceleration of gravity (m/s^2), respectively.

The transmissivity or permeability-thickness (kh) has units of Darcy-metre (Dm).

Davidson and Yu (2008) reports average regional horizontal hydraulic conductivities for the upper 500 m of the Yarragadee aquifer (where most water supply bores are completed) range of 1-3 m/d; equivalent to permeability values of 865-2600 mD, based on the likely groundwater density and viscosity values in the upper part of the aquifer.

Permeability derived from drawdown tests and injection tests of the fourteen selected Perth geothermal bores, some of which are completed deeper, range from 697 to 4,991 mD (average 2,803 mD) and their transmissivities range from 44 to 630 Dm (average 238 Dm).

The values calculated from bore drawdown and injection tests are slightly higher than regional values because the regional values are representative of the entire thickness of the aquifer composed of approximately 50% sandstone beds and 50% siltstone and shale beds whilst geothermal injection bores' screened intervals preferentially exclude siltstone and shale beds.

The porosity-permeability relationship developed of Niederau et al. (2017), derived from Yarragadee core measurements, suggests porosity values for the selected 14 geothermal bores of 25.5-32.5% (average 29.6%) for the high and medium-energy sandstone beds contributing to groundwater flow. This is consistent with the packing porosity limit of about 30% defined by Tait (2008).

Based on the relationship between permeability and pore-throat size developed by Harris and Odom (1982), it is estimated that the pore throat sizes range from 27 to 71 microns (average 51 microns) in the selected 14 geothermal bores' net aquifer intervals.

2.5 Groundwater quality

Groundwater in the Yarragadee aquifer is considerably older than the groundwater in overlying aquifers. This trend is reflected in its groundwater chemistry composition which generally falls on a mixing line between a sodium chloride type and a sodium bicarbonate type (Davidson, 1995).

Groundwater salinities range from fresh to brackish and generally increase with depth and distance from the Gnangara Mound recharge zone situated to the north of Perth (Playford et al., 1976). Based on wireline resistivity data from Cockburn-1 it is estimated that the salinity is about 1 g L^{-1} or less at the top of the aquifer (up to 1100 m depth) and gradually increases to about 30 g L^{-1} at 1300 m depth (Glasson, 2011). Groundwater salinities in the selected 14 bores generally range from 0.5 to 2.0 g L^{-1}.

Dissolved iron from naturally occurring pyrite and siderite minerals within the aquifer is the main element of concern with regards to clogging. This is discussed further in Section 4.

Groundwater is reductive (redox potential of -100 to -150 mV measured in the bores considered for this study). Dissolved gas is limited to small quantities of CO_2 (generally <0.1%).

Water analyses from a selected bore (Bore 10; 812-994 m depth) are provided below.

Alk mg/L	**pH**	**Temp °C**	**EC mS/cm**	**Cl mg/L**	**Na mg/L**	**K mg/L**	**Ca mg/L**	**Mg mg/L**	**SO4 mg/L**	**S mg/L**	**Si mg/L**	**Fe mg/L**
276	7.5	49.8	2.1	434	430	25	8	7	40	13	21	0.05

2.6 Temperature

Ricard et al (2012) show that the average geothermal gradient from surface to 3km in the Perth Basin ranges from 20 to 36.5 °C/km with maximum temperatures ranging from 80 to 130°C at 3km.

The thermal regime underneath Perth is “apparently conductive” with local geographical and depth variation based on a few bore data, and thermal gradient studies (Reid et al., 2011).

There has been some numerical modelling of groundwater flow and heat transport (Reid et al., 2012; Shilling et al., 2013) for the Central Perth Basin. These models have shown the potential influence of faults and advective flows (e.g. recharge of cooler water from overlying aquifers or hotter water via flow from the base of the aquifer) on the temperature distribution both locally and regionally.

Recent drilling and exploration has indeed showed that large temperature variations can occur between areas of up-gradient flow (e.g. Bore 13 - 51°C from 690-958 m depth) and down-gradient flow (e.g. a new water supply bore constructed in early 2018 - 43°C from 870-1282 m) that are only 20-25 km away. This may be indicative that free-convection is occuring in the aquifer as postulated by Niederau et al. (2017) and highligts the importance of continuing to refine the characterisation of the thermal regime of the aquifer.

3. Bore design

3.1 General bore design philosophy

The general bore design philosophy of most geothermal projects in Perth, relies on obtaining preliminary aquifer data via drilling a pilot hole in small diameter, generally 216 mm (8.5 inches), at the start of the project. Pilot hole drilling facilitates data acquisition such as: wireline surveys (GR, resistivity, temperature and sometimes neutron); hydraulic testing of prospective sandstone beds using inflatable packers in the open hole; and Particle Size Distribution (PSD) analyses of the drill cuttings. These data are used to finalise the bore design, in particular the screen setting depth, aperture and length.

Reaming of the pilot hole to a commercial diameter is then undertaken whilst casing and screens are ordered. The intermediate casing is set within a competent low permeability unit near the top of the identified aquifer interval. The intermediate casing is typically 219 mm OD (8.6 inches) 8 mm WT water bore 316L grade stainless steel casing or 244 mm OD (9 5/8 inches) 12 mm WT Cr 13 casing.

Subsequent bore construction stages include pressure cementing of the casing strings, followed by drilling of the shoe track, re-conditioning of the pilot hole below, and installing telescopic standalone wire-wound screens, typically 180 mm OD (7 inches). Screens with an aperture comprised between 350 and 500 microns (depending on PSD analyses) are set across permeable sandstone beds. Zero-aperture screens or 168 mm OD (6.6 inches) 7 mm WT water bore 316 L grade stainless steel blank casing are set across finer-grained sediments.

3.2 Bore hydraulics

In this paper, pressure change in a new bore is expressed using Equation (2) which includes linear and non-linear losses relating to friction losses in the bore casing (Henry and Ramey, 1982).

$$\Delta p = B_{1(rw,t)} \times Q + \left[\frac{Skin}{2\pi Kh} \times \frac{3600 \times 24}{1000} \times Q \right] \times \frac{\rho g}{10^5} + C \times Q^2 \qquad (2)$$

where Δp, $B_{1(rw,t)}$, Skin, Kh, C and Q, are pressure change (bar), linear aquifer loss coefficient (bar/L/s), Skin factor (-), transmissivity or hydraulic conductivity-thickness (m^2/d), non-linear well loss coefficient (bar s^2/L^2) and flow rate (L/s) respectively.

The linear aquifer loss coefficient can be related to the aquifer properties (transmissivity and porosity) and is a function of the bore radius and time. In this paper the coefficient is estimated from the Darcy-pressure drop observed during drawdown and injection tests of the selected bores.

The non-linear well loss coefficient can be related to the bore construction (casing diameter and length). In this paper the coefficient is estimated using the Darcy-Weisbach equation (Rouse, 1946) and a typical friction factor of 0.019.

The Skin factor is iteratively assessed by comparing actual pressure change from drawdown tests of the bores to those predicted from Equation (2). A positive Skin factor suggests extra flow resistance near the borehole wall (i.e. formation damage); a negative skin factor suggests flow enhancement near the borehole wall (i.e. development of the near bore).

The ratio of flow rate to aquifer and skin losses is defined as the Productivity Index (PI).

$$PI = \frac{Q}{\Delta p - C \times Q^2} \qquad (3)$$

The actual PI for the 14 bores in this study (Bore 1 to 14) are shown in Figure 3 below. Values are moderate to high and range from about 5 to 100 L/s / bar. For comparison the theoretical PI values for Skin factors of 0 (i.e. no Skin) and -5 are also presented in Figure 3.

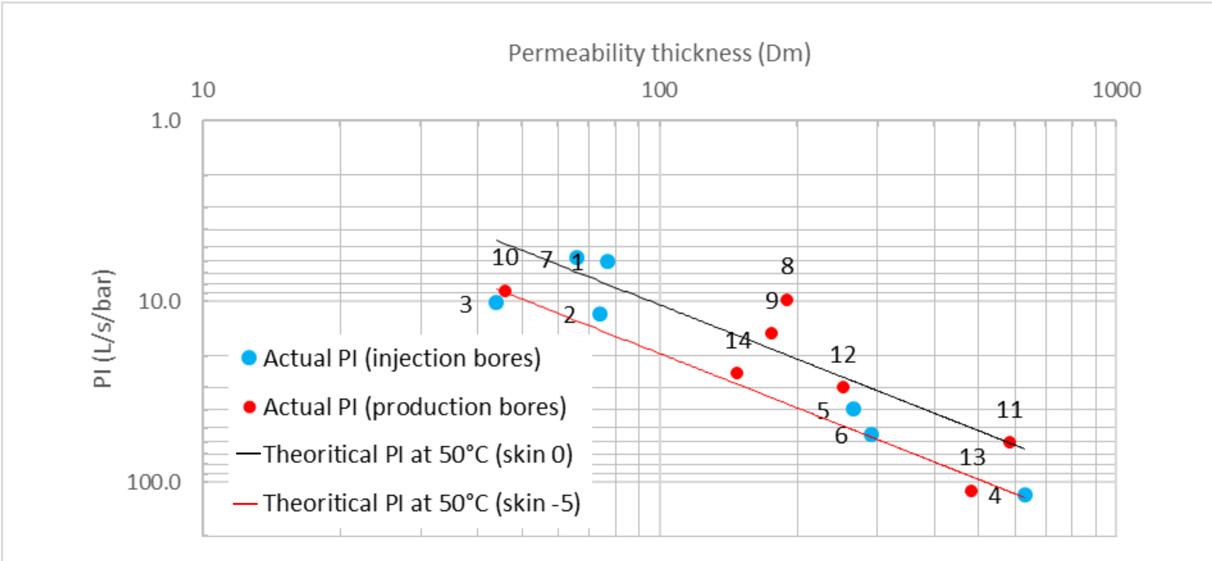

Figure 3: Comparison of actual Productivity Index (PI) with theoretical PI for injection and production bores

Most bores plot below the theoretical curve for +0 Skin factor, indicative of flow enhancement most likely from development. The average Skin factor for those bores is -2.2.

However, positive to neutral skin values (average +2.0) occur in bores 1, 7, 9, 11 and 12. These bores may have been inefficiently developed due to time constraints; or possibly because of a poor screen placement that has led to inefficient packing of formation around the screens. The datum point furthest away from the theoretical curves (Bore 8) corresponds to a bore that had to be perforated and lined with smaller diameter screens (due to ingress of cement grout into the screen interval) and that has a Skin factor of +11.9.

3.3 Sand control

The sand control design philosophy that has been applied to all the selected geothermal bores is based on employing a stand-alone wire-wound screens (without having a gravel packed annulus). Screen aperture sizes are based on the D_{50} or D_{60} of the aquifer open to screens (i.e. 40 to 50% formation retention). However, based on the 1/3 aperture bridging theory (Harris and Odom, 1982) which assumes that particles greater than 1/3 of the aperture will bridge, the actual formation retention is greater.

For example, for the PSD data presented in Figure 2, two screen aperture were considered: (1) 500 microns for the upper part of the formation which has an average D_{60} of 665 microns; and (2) 380 microns for the lower part of the formation which has an average D_{60} of 303 microns.

The 1/3 aperture bridging theory means that formation particles coarser than 167 microns (upper screen) and 127 microns (lower screen) would bridge in the near bore zone providing an effective retention of 85% and 60% of formation respectively.

The actual retention is likely higher, as particles that are comprised of between 1/3 and 1/7 of the apertures may still bridge under low drawdown conditions (i.e. sizes of about 71-167 microns for the upper screen and 54-127 microns for the lower screen). This would provide a theoretical ultimate retention of 90% and 70% of formation respectively. Smaller particles (i.e. finer than 54 microns) are theoretically not retained and able to free flow regardless of the drawdown.

Following screen placement, bores are developed using combined jetting and airlifting methods for up to 100 hours or until the Total Suspended Solids (TSS) concentration in the pumped groundwater is less than 5 mg/L when possible. This allows free-flowing particles (i.e. that did not bridge in the near bore zone) to be flushed through the screens and into the bore enhancing the near-bore zone porosity and Skin factors. As shown in Figure 3 this results in negative Skin factors for most of the bores.

3.4 Velocities

For comparison purposes as proposed by Pyne (2005) we refer to normalised borehole wall velocities of 3 feet/hour or about 0.025 cm/s. This is the flow rate divided by the infiltration surface area. Bores selected have a borehole wall velocity ranging from 0.030 to 0.088 cm/s.

Other authors (Ungemach, 2003) refer to the sandface velocity at the pore level which is higher than the borehole wall velocities because only about 30% of the borehole wall surface area contribute to flow (i.e. flow occurs is through the porosity volume of the formation). In line with the commonly accepted industry practice, the bore designs allow for a maximum sandface velocity of 1 cm/s at the screen/aquifer interface (Ungemach, 2003) which corresponds to the transition to turbulent flow regime Reynolds number (Re) > 2000 within a typical pore throat size of 100 microns. Low sandface velocities can reduce the potential for sand pumping in standalone screen completion. For the selected bores the sandface velocity at maximum flow rate is calculated to range from 0.11 cm/s to 0.25 cm/s (0.17 cm/s on average). Given the estimated pore throat sizes of 26 to 71 microns, this is equivalent to Reynolds numbers ranging from 93 to 351 well below the threshold for fully turbulent flow (Re = 2000) but above laminar conditions (Re = 10).

To mitigate the potential for turbulent flow and screen erosion, a screen entrance maximum velocity criteria of 3 cm/s is adopted as recommended by the leading screen suppliers (Sterett, 2007). For the selected bores the screen entrance velocity is calculated to range from 0.35 to 1.20 cm/s.

4. Surface design

4.1 Filtering of free-flowing solids

Apart from one production bore (Bore 8) that is operating at fairly low flows (12 L/s), all the other geothermal production bores (Bores 9 to 14) employ some form of surface filtration to reduce the TSS prior to injection.

For operational efficiency and ease of maintenance, filtering is undertaken using automatic backwashing mechanical filters with screen sizes ranging from 25 to 100 microns. These filters operate under minimum positive pressures of 2-3 bars and the geothermal fluid does not get into contact with air which has been found to mitigate risks associated with dissolved iron precipitating as iron oxi-hydroxide. Dissolved iron can be naturally present in the water or a consequence from minor corrosion of the bore casing.

The primary function of the filter is to protect heat exchangers and filter the coarser fraction of solids that are free-flowing through the standalone screens.

As discussed in Section 3.2 based on PSD data for Bore 13, free-flowing solids can be up to 167 microns in size for a common 500 microns screen aperture under a high drawdown scenario and up to 54 microns for a smaller screen aperture size of 380 microns and a low drawdown scenario.

Suspended solids analyses were undertaken for the six production bores that employ surface filtration (i.e. bores 9 to 14). Pre-filtration, the measured TSS is less than 5 mg/L for most bores (Bores 9, 11, 12 and 13) but is higher than 5 mg/L in two of the tested bores (Bores 10 and 14).

Maximum particle sizes for the three bores with the three highest TSS values (Bores 9, 10, 14) are 300, 399 and 157 microns respectively close to (and even exceeding) the calculated maximum free-flowing particle size value calculated in Section 3.2. The maximum particle sizes for the bores with low TSS range from 20 to 50 microns close to the minimum free-flowing particle size value calculated in Section 3.2 for a low drawdown scenario.

Measured TSS concentrations were correlated to the permeability in Figure 4. The results suggest that there is a strong correlation between concentration of free-flowing particles and low permeability. This is consistent with the sand control concepts discussed previously which assume that under a high drawdown scenario (i.e. or low permeability) coarser particulates are likely to flow through the screens resulting in a higher TSS.

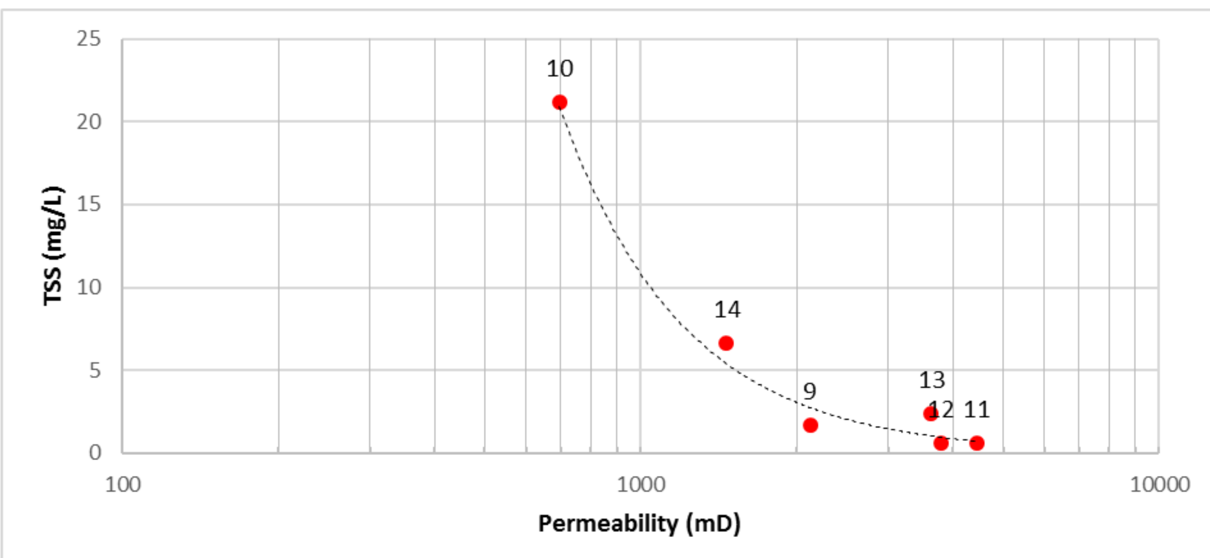

Figure 4: Correlation between TSS and permeability for production bores

After filtration, the TSS is reduced to less than 5 mg/L (average 1.9 mg/L) for all bores confirming the benefit of surface filtration prior to injection, particularly where high TSS occur and particle sizes are greater than the filtration size. Particle sizes post-filtration range from 25 to 100 microns depending on the filtration system adopted.

Based on the pore throat sizes of 26 to 71 microns estimated previously using the relationship developed by Harris and Odom (1982) and the 1/3 bridging theory, it is predicted that filtration to about 5 microns (low permeability injection bores) and 25 microns (high permeability injection bores) would be necessary to prevent the plugging of pores and subsequent clogging. Given that the particle sizes post filtration range from 25 to 100 microns, it is therefore likely that clogging through suspended particles will occur, particularly where particle sizes are in excess of 25 microns and the injection bore has low permeability.

However, it appears that minimal benefit with regards to clogging is provided for high permeability bores that already have low TSS (< 5 mg/L) and pore throat size exceeding particle sizes post-filtration.

4.2 Injection control

The Yarragadee aquifer pressures have declined significantly since the early 20th century, primarily because of its exploitation for public water supplies. Currently, the pressure is declining by 1-2 bar every 10 years.

As a result, the aquifer is no longer artesian in Perth and the static potentiometric surface is up to 80 m depth in the north western suburbs where ground elevations can be up to 50 m above the sea level. Therefore, the estimated injection head, including friction, aquifer and clogging losses is often insufficient for a positive injection pressure to be registered at the injection borehead when the bores are first used, particularly for bores with a high PI. This increase the potential for air entrainment as vacuum conditions can develop in the pipework; eventually allowing air/water contact and air entrainment. Air/water contact can lead to iron oxi-hydroxide precipitation (Warner, 1966) while air bubbles can lead to rapid blocking of the formation pores (Sniegocki, 1963).

Air entrainment has generally been prevented by using downhole injection control valves or a Pressure Sustaining Valve (PSV) that create the necessary friction losses to maintain a minimum injection pressure in the surface pipework (typically 2 bar). While air entrainment occurred in early projects this is now generally well mitigated in new projects.

4.3 Injection pressure

The injection pressure in a bore is given by Equation (3).

$$p_i = MAX(\Delta p_i - SWL \times \frac{\rho g}{10^5}, p_{PSV}) \quad (3)$$

where Δpi, SWL and p_{PSV} are the injection pressure change (bar) static water level (m) and PSV target surface injection pressure (bar) respectively.

There is little published information on the fracture gradient in the Yarragadee aquifer. However, from unpublished Leak-off Test data collected as part of a recent drilling program targeting the formation in the Greater Perth region, it is believed that the fracture gradient may be exceed 1.7 bar/ 10 m. Given a normal hydrostatic gradient of 0.98 bar / 10 m, this provides the maximum allowable surface injection pressure to prevent hydraulic fracturing of about 0.7 bar / 10 m.

For a typical depth of 500 m to the top of the injection zone and a safety factor of about 75%, this gives a maximum injection pressure of up to about 20 bar.

In practice the maximum operating pressure of Perth geothermal systems is generally 10 bar as per the pressure rating of the filter and heat exchanger infrastructure. As project scale increase it may be possible to envisage using an injection pump so that plant room pressure can remain below 10 bar while injection pressure are raised to up to 20 bar if required.

For a typical Static Water Level (SWL) of 50 m and a maximum surface operating pressure of 10 bar, it is estimated that the maximum allowable injection pressure change before cleaning of the injection bore is required is 15 bar. Where the original injection pressure is 3 bar and redevelopment is not to occur more often than 3 or 5 years (to maintain acceptable operating costs), the maximum desired injection pressure increase through clogging is about 4 bar/year and about 2.5 bar/year respectively.

5. Clogging in injection bores

5.1 Clogging rates

The pressure change in an injection bore after a period, t is a combination of aquifer, friction and clogging losses. In this paper, injection pressure change is expressed using Equation (4)

$$\Delta p_i = B_{1(rw,t)} \times Q_i + C \times Q_i^2 + \left[\frac{Skin}{2\pi Kh} \times \frac{3600 \times 24}{1000} \times Q_i \right] \times \frac{\rho g}{10^5} + \Phi_{(t,Q)} \qquad (4)$$

where $\Phi_{(t,Q)}$, Q_i and t, are the clogging losses (bar) injection flow rate (L/s) and period of measurement (years) respectively.

The clogging rate is calculated using Equation (5)

$$\Delta\Phi = \frac{\Phi_{(t,Q)}}{t} \times 365 = \frac{p_i - B_{1(rw,t)} \times Q_i - \left[\frac{Skin}{2\pi Kh} \times \frac{3600 \times 24}{1000} \times Q_i \right] \times \frac{\rho g}{10^5} - C \times Q_i^2}{t} \times 365 \qquad (5)$$

The annual clogging rates for the seven selected injection bores (Bore 1 to 7) range from 0.1 bar to up to 9 bar. However, the clogging rates are not directly comparable given that flow-rates are different for each bore.

5.2 Normalisation of clogging rates

In this paper we follow the usage of Pyne (2005) who uses a standard flux at the borehole wall and a standard temperature to normalise injection bore clogging data to allow for a more meaningful comparison of clogging rates. The following Equation (modified from Oolsthorn, 1982) is used to calculate normalised clogging rates.

$$\Delta\Phi_{norm} = \Delta\Phi\left(\frac{v_s}{v}\right)\left(\frac{\mu_s}{\mu}\right)\left(\frac{v_s}{v_{avg}}\right) \tag{5}$$

Where v_x, v, v_{avg} and μ_s are the standard 0.025 cm/s borehole wall velocity (cm/s), the actual velocity (cm/s) when clogging is assessed (typically at maximum flow rate), the average velocity (cm/s) when the system is operating which is generally less than the max velocity given that the geothermal heating load varies throughout the year and the standard viscosity (cP) for a standard injection temperature of 35°C.

Normalised clogging rates are not necessarily estimates of actual clogging rates under those conditions, but are meant to adjust for various injection bore clogging examples for comparison purposes. Normalised clogging rates for the seven selected injection bores range from 0 to 1.4 bar.

In the Sections below we attempt to correlate normalised clogging rates with some of the parameters discussed in Sections 2, 3 and 4 to identify the key parameters that affect clogging rates.

5.3 Correlation with permeability

In Figure 5, the normalised clogging rate is correlated to the permeability. Low rates of clogging (<0.5 bar/year) are shown for bores (1, 2, 4, 5 and 6) with a permeability higher than 1,000 mD. However, for bores with lower permeabilities (bore 3 and 7) the clogging rate increase very rapidly. This is possibly a consequence of the lower pore throat size in less permeable sandstones which increase the potential for suspended solids to bridge leading to formation of a filter cake at the sandface and increased clogging rate. In more permeable bore suspended solids in the injection water are more likely to free flow without bridging at the sandface.

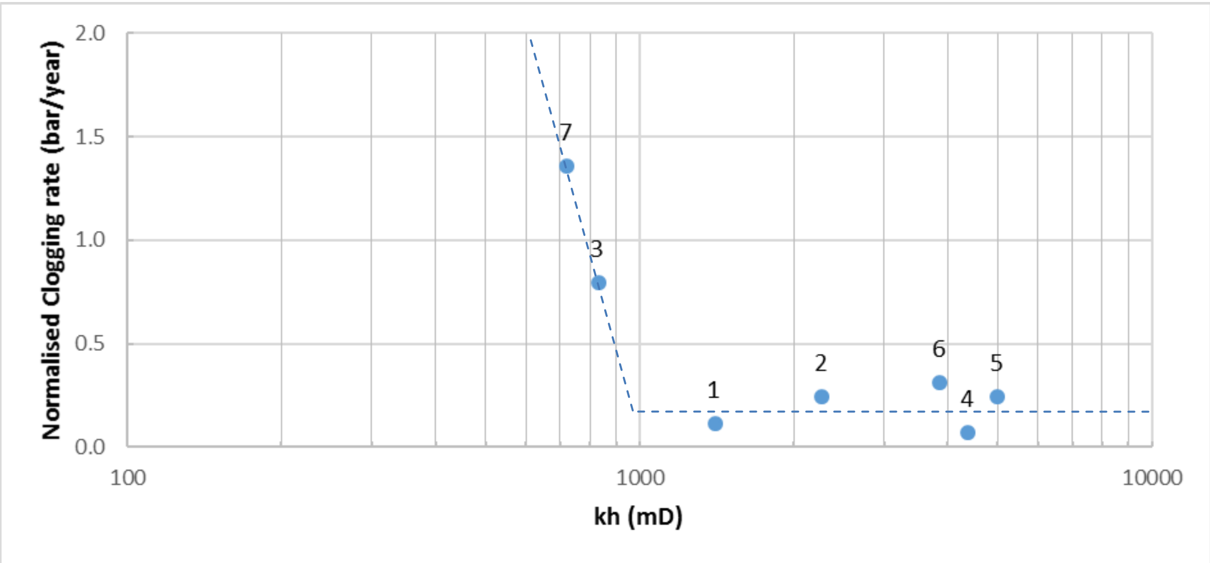

Figure 5: Correlation clogging rate and permeability for injection bores

The slightly higher clogging rate observed in Bore 6 is likely to be due to other factors. It is postulated that in this bore the particularly deep SWL of 80 m may have increased the potential for air entrainment and associated additional clogging. The latter is consistent with the requirement to replace the injection control packer during the period of review for this bore.

5.4 Correlation with flow rate per metre of net aquifer

In Figure 6, the normalised clogging rate is correlated to the flow rate per metre of net aquifer. There is an acceptable correlation showing higher rates of clogging where flow rate per metre of net aquifer are high, however, as shown above the behavior is different for permeable and less permeable bores.

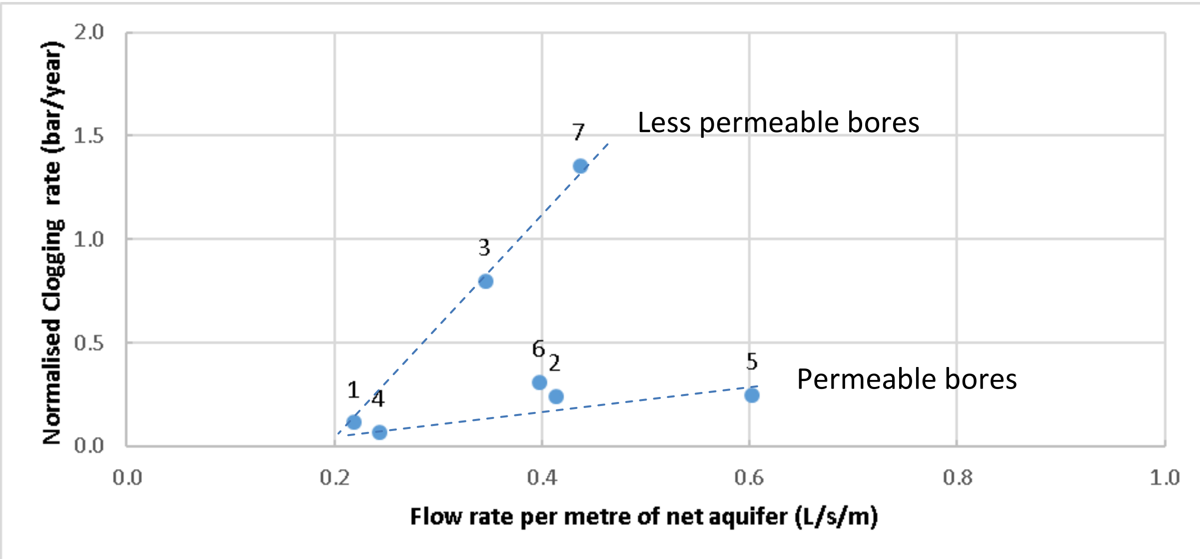

Figure 6: Correlation clogging rate and flow rate per metre of net aquifer for injection bores

In permeable bores (bores 2, 4, 5 and 6) clogging rates increase slower with an increase in flow rate per metre of net aquifer while in less permeable bores clogging rates (bore 1, 3, and 7) increase faster. This plot provides practical criteria for minimising clogging rate that can be rapidly utilised in the field after the available net aquifer thicknesses have been estimated in the pilot hole (eg longer screen interval).

5.5 Correlation with TSS post-filter

In Figure 7, the normalised clogging rate is correlated to the TSS post-filter.

There is an acceptable correlation showing higher rate of clogging where TSS concentrations are high, however, as discussed the behavior is different for permeable and less permeable bores. In permeable bores (bores 2, 4, 5 and 6) clogging rates increase more slowly with the TSS while in less permeable bores clogging rates (bore 3, and 7) increase faster.

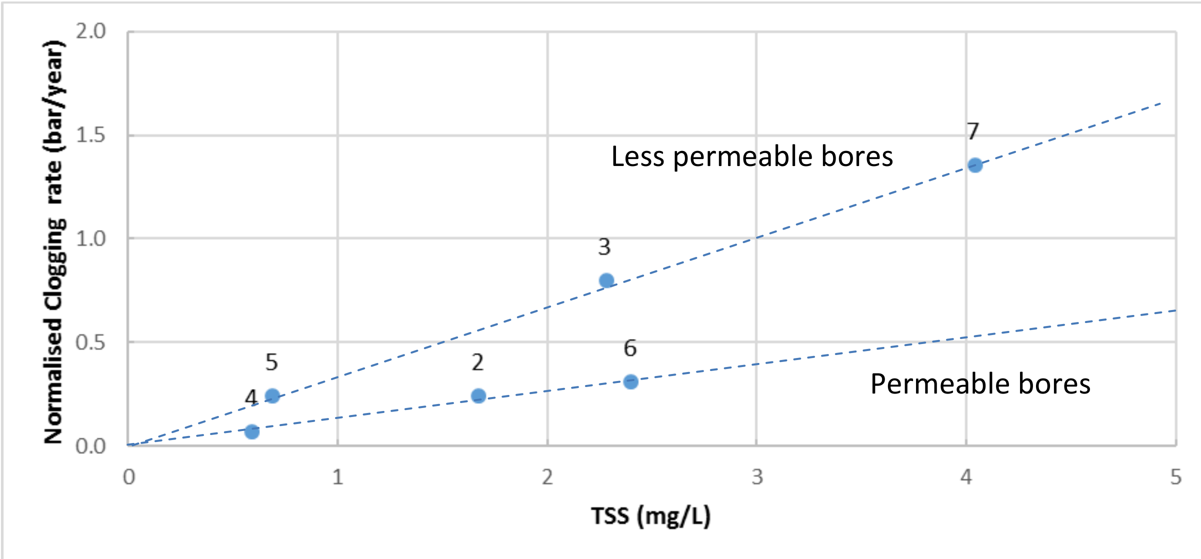

Figure 7: Correlation clogging rate and TSS post filter for injection bores

5.6 Correlation with Reynolds number

In Figure 8, the actual clogging rate (i.e. not normalised) is correlated to the Reynolds number which is dependent on the sandface velocity as we have seen in Section 3.3. There is a good correlation showing higher rates of clogging where the Reynolds number (and also the sandface velocity) is higher. The data below suggests that using the industry accepted Reynolds number of 2000 for production bores (equivalent to a sandface velocity of 1 cm/s in 100 microns pore throat or 0.5 cm/s in 50 microns pore throat) when designing injection bores could lead to excessive clogging. A Reynolds criterion of 125 might be more suitable for conservative injection bore design for less permeable bores. For more permeable bores a Reynolds number of 400 may be suitable.

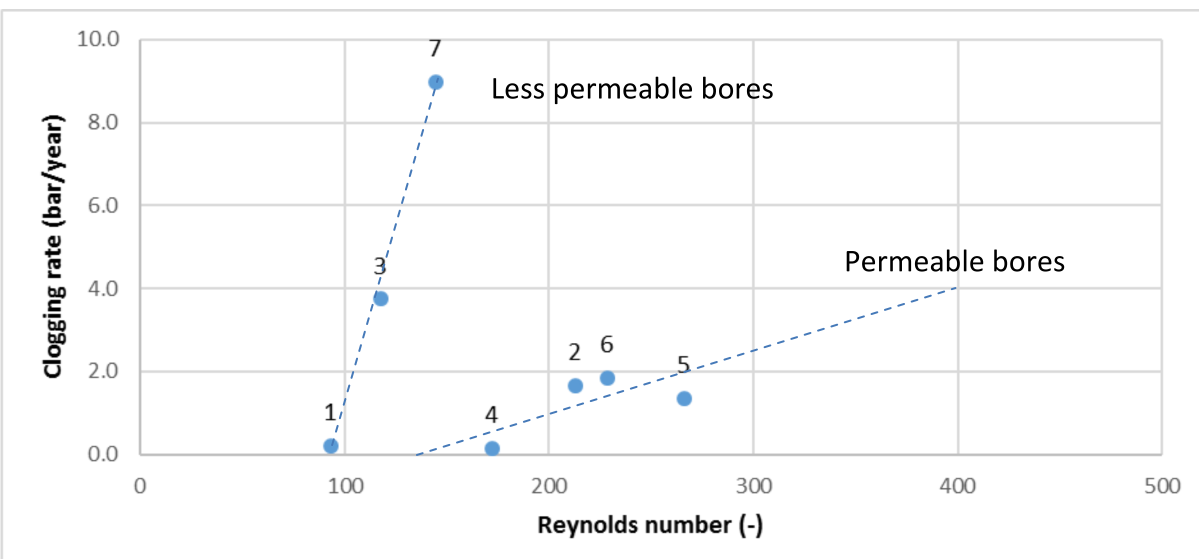

Figure 8: Correlation clogging rate and sandface velocity for injection bores

6. Conclusion

Over the last 20 years the Yarragadee sandstone aquifer has been targeted by 14 geothermal projects that involve the injection of large volumes of heat-depleted groundwater in Perth. These projects have largely avoided the severe clogging issues that have impeded the development of many clastic geothermal resources globally. However, some injection bores have experienced higher clogging rates and have undergone regular injection bore cleaning workovers (ie redevelopment) to maintain sufficiently injectivity values (and thus acceptable operating costs).

A review of seven selected geothermal projects has been undertaken to identify the key parameters and methodologies that have helped minimising clogging when injecting heat-depleted water in Perth’s Yarragadee sandstone aquifer.

The review shows that for typical standalone wire-wound screen bore completions, Total Suspended Solids concentrations are correlated to the permeability of the sandstone interval targeted. Solid concentrations in less permeable bores (k < 1500 mD) can be in excess of 5 mg/L whilst more permeable bores typically have lower solids concentration.

Produced solids concentrations are reduced to about 2 mg/L after surface filtration through automatic backwashing 25-100 microns filters. This level of filtration is generally sufficient to prevent clogging in the most permeable bores (i.e. k = 5000 mD) which have pore throat sizes of up to 75 microns. However, some form of pore plugging and wellbore narrowing occurs in less permeable bores.

Results presented in this paper show that the clogging rates can be effectively mitigated by:

- Targeting permeabilities greater than 1500 mD (with associated pore throat sizes of about 32 microns) for production bore-screened intervals; and/or
- Limiting the flow rate per metre of net aquifer to about 0.3 L/s / m in less permeable injection bores (eg greater screen interval) and 0.7 L/s / m in permeable injection bores; and/or
- Filtering to 5 microns and 1.5 mg/L TSS when injecting into less permeable bores and 25 microns and 5 mg/L TSS when injecting in permeable bores; and/or
- Considering filter pack completions for less-permeable production bores to reduce the necessary amount of surface filtration; and/or
- Adopting a design sandface criteria of 0.2 cm/s for less permeable bores (Re < 125) and 0.3 cm/s (Re < 400) for permeable bores.

Where significant clogging occurs, regular bore cleaning workover (ie bore redevelopment) are generally sufficient to restore original injectivity. Redevelopment methods must target the key clogging mechanisms (usually plugging of bores and wellbore narrowing but also iron oxide deposits and or air bubbles blocking the pores in some cases).

The results presented in this paper confirm that the Yarragadee aquifer is well suited for geothermal applications and are encouraging for the development and scaling up of the industry. The assessment methodology is applicable to other clastic geothermal plays globally.

REFERENCES

Corbett, P. W. M. et al. “Layered fluvial reservoirs with internal fluid cross flow: a well-connected family of well test pressure transient responses”, Petroleum Geoscience,18(2):219, 2012.

Davidson, WA. “Hydrogeology and groundwater resources of the Perth region”, Western Australia. Geological Survey of WA, 1995.

Davidson WA, Yu X. “Perth regional aquifer modelling system (PRAMS) model development: Hydrogeology and groundwater modelling”, Department of Water, 2008.

Delle Piane, C., Esteban, L., Timms, N. E. and Ramesh Israni. S, “Physical properties of Mesozoic sedimentary rocks from the Perth Basin, Western Australia”, Australian Journal of Earth Sciences 60, (6-7): 735-745, 2013.

Glasson, S., “ Investigation of salinity within the Yarragadee Aquifer in the Perth area”, BoE diss., University of Western Australia, 2011.

Harris C, Odom C. “Effective filtration in completion and other wellbore operations can be good investment”, Oil Gas J.;(United States), Sep 20;80(38), 1982.

Henry JR, J. Ramey. "Well—Loss Function and the Skin Effect: A Review", Recent trends in hydrogeology, 189 (1982): 265, 1982.

Niederau J, Ebigbo A, Marquart G, Arnold J, Clauser C. “On the impact of spatially heterogenous permeability on free convection in the Perth Basin, Australia”, Geothermics. 2017 Mar 1;66:119-33, 2017.

Oolsthoorn, T. N. "The clogging of recharge wells.", KIWA-communications, 72. Risjwikn, Netherlands Waterworks Testing and Research Institute (1982), 1982.

Playford PE, Low GH, Cockbain AE. “Geology of the Perth Basin, Western Australia”, Geological Survey of Western Australia, 1976.

Pujol M, Ricard LP, Bolton G. “20 years of exploitation of the Yarragadee aquifer in the Perth Basin of Western Australia for direct-use of geothermal heat”, Geothermics. 2015 Sep 1;57:39-55, 2015.

Pyne RD. :Aquifer storage recovery: a guide to groundwater recharge through wells”, ASR systems, 2005.

Reid, L.B., Bloomfield, G., Botman, C., Ricard, L., Wilkes, P., 2011. Temperature Regime in the Perth Metropolitan Area: Results of Temperature and Gamma Logging and Analysis, June/July 20110. CSIRO Report.

Reid, L.B., Corbel, S., Poulet, T., Ricard, L.P., Schilling, O., Sheldon, H.A., Wellmann, J.F., 2012 Hydrothermal modelling in the Perth Basin, Western Australia.

Ricard L. P., Trefry, M. G., Reid, L. B., Corbel, S., Esteban, L., Chanu, J.-B., Wilkes, P. G., Douglas, G. B., Kaksonen, A. H., Lester, D. R., Metcalfe, G. P., Pimienta, L., Gutbrodt, S., Tressler, S. Bloomfield, G., Evans, C. and Regenauer-Lieb, K. (2012). Productivity and sustainability of low-temperature geothermal resources. Final Report of Project 4, Perth Basin Assessments Program, Western Australian Geothermal Centre of Excellence, Report EP122629, April 2012.Rouse, H., “Elementary Mechanics of Fluids”, John Wiley and Sons, New York, 1946.

Schilling, O., Sheldon, H.A., Reid, L.B., Corbel, S., 2013. Hydrothermal models of the Perth Metropolitan Area, Western Australia: implications for geothermal energy. Hydrogeol. J. 21 (3), 605-621.

Sniegocki R. T., “Problems in Artificial Recharge through Wells in the Grand-Prairie Region Arkansas”, Water-supply Paper, 1615-F, Washington, USGS, 1963.

Tait, A., “A study of the Yarragadee Formation based on cores from Cockburn 1, Gage Roads 1, Gingin 1, Quinns Rock 1, Sugarloaf 1, Warnbro 1 and Whicher Range 1”, WA Department of Industry and Resources Approvals: S31910 and S31927, 2008.

Timms, N., Corbel, S., Olierook, H., Wilkes, P., Delle Piane, C., Sheldon, H., Alix, R., Horowitz, F., Wilson, M., Evans, K. A., Griffiths, C., Stütenbecker, L., Israni, S., Hamilton, J., Esteban, L., Cope, P., Evans, C., Pimienta, L., Dyt, C., Huang, X., Hopkins, J., and Champion, D., “A new understanding of the Perth Basin for geothermal exploration”, WA Geothermal Centre of Excellence, 2012.

Ungemach, P., “Reinjection of cooled geothermal brines into sandstone reservoirs.”, Geothermics 32, 4: 743-761, 2003

Warner D. L., “Deep Well Waste Injection, Recation with aquifer water”, Journ. Of the Dan. Eng. Div. August, pp 45-69, 1966.

APPENDIX I: KEY BORE DATA

Bore ID	Type	Screens	Net aquifer	k	Flow / m	TSS	Reynolds	Δϕ	Δϕnorm
		m	*m*	*mD*	*L/s / m*	*mg/L*	*-*	*bar/year*	*bar/year*
1	i	524-609	54.9	1403	0.22	N/D	93	0.2	0.1
2	i	540-600	32.6	2270	0.41	1.7	213	1.7	0.2
3	i	488-682	53.0	831	0.35	2.3	117	3.7	0.8
4	i	593-797	143.8	4381	0.24	0.6	172	0.1	0.1
5	i	360-474	53.1	4991	0.60	0.7	266	1.4	0.2
6	i	288-429.5	75.4	3859	0.40	2.4	228	1.9	0.3
7	i	527-780	91.6	721	0.44	4.0	145	9.0	1.4
8	p	669-732	41.3	4630	0.29	N/D	180	N/A	N/A
9	p	670-856	83.2	2121	0.16	1.7	123	N/A	N/A
10	p	812-994	66.0	697	0.28	21.2	112	N/A	N/A
11	p	944-1154	131.3	4448	0.27	0.6	224	N/A	N/A
12	p	833-971	66.6	3799	0.48	0.6	351	N/A	N/A
13	p	690-958	133.0	3633	0.23	2.4	200	N/A	N/A
14	p	811-1024	101.5	1463	0.39	6.6	199	N/A	N/A

i:Injection Bore p:Production Bore